A. M. J. Spits, Nucl. Phys. A113, 395 (1968).
[6]H. T. Fortune, R. C. Bearse, G. C. Morrison, J. L. Yntema, and B. H. Wildenthal, Bull. Am. Phys. Soc. 15, 483 (1970); and to be published.
[7]P. A. Quin and S. E. Vigdor, Bull. Am. Phys. Soc. 15, 1686 (1970); and to be published.
[8]E. C. Halbert, J. B. McGrory, B. H. Wildenthal, and S. P. Pandya, to be published.
[9]R. R. Betts, H. T. Fortune, J. D. Garrett, R. Middleton, D. J. Pullen, and O. Hansen, Phys. Rev. Letters 26, 1121 (1971).
[10]R. Middleton, in *Proceedings of the International Conference on Nuclear Reactions Induced by Heavy Ions, Heidelberg, Germany, 1969,* edited by R. Bock and W. R. Hering (North-Holland Publishing Company, Amsterdam, The Netherlands, 1970), p. 263.
[11]M. A. Spivack, Rev. Sci. Instr. 41, 1614 (1970).
[12]B. H. Wildenthal, private communication.

PHYSICAL REVIEW C VOLUME 4, NUMBER 3 SEPTEMBER 1971

Reaction Matrix Elements and Structure Calculations with the Yale and Reid Potentials for the Ni Region*

M. L. Rustgi, H. W. Kung, R. Raj, R. A. Nisley, and M. H. Hull, Jr.
Nuclear Physics Laboratory, Department of Physics, State University of New York, Buffalo, New York 14214
(Received 19 April 1971)

Employing the Yale and soft-core Reid free nucleon-nucleon potentials, the shell-model reaction matrix elements are calculated and tabulated for the Ni region. The matrix elements consist of the bare part and the renormalization effects due to the core polarization. The bare matrix elements are evaluated following the unitary-model approach of Shakin, Waghmare, Tomaselli, and Hull and the renormalization corrections are calculated in the same manner as by Kuo and Brown for a Ni^{56} core. As a test of these matrix elements, spherical shell-model spectra of Ni^{58}, Cu^{58}, Ni^{59}, Cu^{59}, Ni^{60}, Zn^{60}, and Cu^{60} are calculated. Quasiparticle calculations for the odd and even Ni isotopes are also performed. In general the calculated results are in good agreement with each other as well as with the observed data. It is concluded that different potentials which fit the same nucleon-nucleon scattering data give essentially the same results for effective-interaction and nuclear-structure calculations for the Ni region of the Periodic Table.

I. INTRODUCTION

In the last decade considerable effort had been spent in developing improved techniques suitable for calculating the spectra of finite nuclei from first principles using a nucleon-nucleon interaction which fits all the available elastic scattering data and the ground-state properties of the deuteron. One of the more successful approaches has been the one developed by Brueckner for nuclear-matter calculations and adopted by Kuo and Brown[1] for finite nuclei. The lowest-order term in the reaction matrix was first used in an effective-interaction calculation by Dawson, Talmi, and Walecka.[2] In their publications,[1,3] Kuo and Brown have used the excited configurations of the inert core to renormalize the matrix elements. The significance of the core-polarization diagram was first pointed out by Bertsch.[4]

Another approach, which has not received much attention, has been developed by Bell[5] and Villars.[6] In this method one introduces a unitary transformation, which operating on a shell-model wave function has the effect of introducing short-range correlations of the type discussed by Gomes, Walecka, and Weisskopf.[7] These correlations are produced by the Pauli principle as well as by the strongly repulsive character of the short-range part of the two-nucleon force.

Employing the unitary-model operator approach, Shakin, Waghmare, Tomaselli, and Hull[8,9] (SWTH) have calculated the effective interactions for the s-d shell region of the Periodic Table employing the Yale potential.[10] These interactions have been used by Pal and Stamp[11] and numerous other workers in describing the nuclear properties and spectra of the $N=Z$ nuclei. Though the treatment of Kuo and Brown and SWTH look different in appearance, the resulting equations look as if they had come out of a Brueckner treatment.

In the work of SWTH, the treatment of the tensor force also does not differ significantly except that no attempt is made to couple D waves with S waves in the short-range correlated wave function; the coupling is included entirely in the long-range part of the interaction. A special feature of the work of SWTH is the use of pseudopotentials to make the separation method applicable to P waves.

Employing the renormalized matrix elements of Hamada-Johnston (HJ) interaction, shell-model

calculations of those nuclei whose wave functions predominantly contain two nucleons plus an inert core have been carried out by Kuo and Brown. Similar calculations with the Tabakin potential have been performed by Kuo, Baranger, and Baranger.[12] The agreement with the experimental data is truly impressive and has encouraged more complicated calculations with several nucleons outside the closed core, especially in the Ni region.[13-15]

In the present paper the reaction matrix elements corresponding to the Yale[10] (Y) and soft-core Reid (R) potentials[16] are calculated for the Ni region following the procedure of SWTH and the core-polarization corrections are calculated following the work of Kuo and Brown. The matrix elements are then used to calculate the shell-model spectra of Ni^{58}, Cu^{58}, Ni^{59}, Cu^{59}, Ni^{60}, Cu^{60}, Zn^{60}, and the spectra of all even and odd Ni isotopes within the modified Tamm-Dancoff-approximation (MTDA) method following the work of Pal and collaborators.[17,18] When compared with the previous results obtained with the HJ interaction,[13-15] no significant differences in the matrix elements and spectra are found suggesting that different potentials which fit the same two-nucleon scattering data give essentially the same results in the Ni region of the Periodic Table.

A major drawback of these structure calculations, as also of all other similar ones, is that the single-particle energies are not determined in a self-consistent manner. The unperturbed single-particle energies for the orbitals $1p_{3/2}$, $0f_{5/2}$, and $1p_{1/2}$ are taken to be 0.0, 0.78, and 1.08 MeV, respectively, from the Ni^{57} spectrum. The unperturbed single-particle energy for $0g_{9/2}$ is taken to be 5.0 MeV, and is the same as used in Refs. 13-15.

II. CALCULATION OF MATRIX ELEMENTS

As has been mentioned in the Introduction, we shall follow SWTH to derive the effective-interaction matrix elements and avoid solving the full Brueckner-Bethe-Goldstone equation for finite systems. Their procedure is briefly outlined here.

The fundamental matrix element between properly normalized and antisymmetrized two-body states is

$$\begin{aligned}
&\langle n_1(l_1\tfrac{1}{2})j_1, n_2(l_2\tfrac{1}{2})j_2 | V_{\rm eff} | n_3(l_3\tfrac{1}{2})j_3, n_4(l_4\tfrac{1}{2})j_4\rangle_{JT} \\
&= [(1+\delta_{n_1n_2}\delta_{l_1l_2}\delta_{j_1j_2})(1+\delta_{n_3n_4}\delta_{l_3l_4}\delta_{j_3j_4})]^{-1/2} \sum_{\substack{\lambda\lambda' J' nn' \\ ll' NLS}} (-)^{\lambda+\lambda'}(2J'+1)(2\lambda+1)(2\lambda'+1)(2S+1) \\
&\times [(2j_1+1)(2j_2+1)(2j_3+1)(2j_4+1)]^{1/2} \langle n_1 l_1 n_2 l_2 \lambda | nlNL\lambda\rangle \langle n_3 l_3 n_4 l_4 \lambda' | n' l' NL\lambda'\rangle \\
&\times \begin{Bmatrix} L & l' & \lambda' \\ S & J & J' \end{Bmatrix} \begin{Bmatrix} L & l & \lambda \\ S & J & J' \end{Bmatrix} \begin{Bmatrix} l_1 & l_2 & \lambda' \\ \frac{1}{2} & \frac{1}{2} & S \\ j_1 & j_2 & J \end{Bmatrix} \begin{Bmatrix} l_3 & l_4 & \lambda' \\ \frac{1}{2} & \frac{1}{2} & S \\ j_3 & j_4 & J \end{Bmatrix} [1-(-)^{l+S+T}] \langle (nl,S)J' | V_{\rm eff} | (n' l', S)J'\rangle ,
\end{aligned} \tag{1}$$

where the curly braces represent the 6-j and 9-j symbols, $\langle n_1 l_1 n_2 l_2 \lambda | nlNL\lambda\rangle$ denote the Moshinsky brackets,[19] and the interaction has been assumed to be independent of the center-of-mass coordinates. The relative matrix elements are

$$\langle (nl,S)J' | v_{\rm eff} | (n'l',S)J'\rangle = {}_c\langle (nl,S)J' | V^{(1)} + V^{(2)} | (n'l',S)J'\rangle_c , \tag{2}$$

$$V^{(1)} = v^{\rm L} - VP + v_{\rm T}^{\rm OD} , \tag{3}$$

$$V^{(2)} = -(v^{\rm L} - VP)\frac{Q}{e}(v^{\rm L} - VP) - v_{\rm T}^{\rm OD}\frac{Q}{e}v_{\rm T}^{\rm OD} , \tag{4}$$

where $v^{\rm L}$ is the long-range part of the two-body interaction diagonal in the orbital angular momentum l; $v_{\rm T}^{\rm OD}$ is the component of the tensor force off-diagonal in l; Q is the Pauli operator and e the energy denominator. The states $|(nl,S)_j\rangle_c$ are the correlated relative states of SWTH governed by the following equations:

$$[t_r + u(r) + v^{\rm S} + VP]|(nl,S)J'\rangle_c = \hbar\omega(2n+l+\tfrac{3}{2})|(nl,S)J'\rangle_c , \tag{5}$$

$$(t_r + u(r)|(nl,S)J'\rangle = \hbar\omega(2n+l+\tfrac{3}{2})|(nl,S)J'\rangle , \tag{6}$$

$$u(r) = \tfrac{1}{2}kr^2 . \tag{7}$$

TABLE I. Reaction matrix elements for the Yale and Reid potentials with Ni^{56} as the core. The symbols a, b, c and d denote the angular momenta which occur in any given matrix element. The shell-model orbits $1p_{3/2}$, $0f_{5/2}$, $1p_{1/2}$, and $g_{9/2}$ are labeled by numbers 8, 9, 10, and 11. The bare matrix elements are denoted by G and Sum includes the contributions of the three-particle–one-hole, two-particle, and two-hole corrections to G.

						Reid pot.		Yale pot.	
T	a	b	c	d	J	Sum	G	Sum	G
0	8	8	8	8	1	−0.8919	−0.6338	−1.0175	−0.7863
0	8	8	8	9	1	0.2386	0.0133	0.2930	0.0652
0	8	8	8	10	1	1.1208	1.3677	1.0049	1.2892
0	8	8	9	9	1	0.1200	0.0376	0.1112	−0.0122
0	8	8	10	10	1	0.1102	0.6054	−0.0668	0.4743
0	8	8	11	11	1	0.5490	0.1141	0.3947	−0.0488
0	8	9	8	9	1	−2.0573	−1.8030	−2.1855	−1.8459
0	8	9	8	10	1	−0.9152	−0.4498	−1.0382	−0.5445
0	8	9	9	9	1	0.6411	0.2986	0.7421	0.3032
0	8	9	10	10	1	0.3987	0.4288	0.4359	0.4413
0	8	9	11	11	1	0.3905	0.1392	0.3190	0.0685
0	8	10	8	10	1	−2.3781	−1.9874	−2.5215	−2.1547
0	8	10	9	9	1	−0.0945	0.2429	−0.1504	0.2153
0	8	10	10	10	1	0.4694	0.4390	0.4632	0.4453
0	8	10	11	11	1	−0.4172	−0.3098	−0.3700	−0.2829
0	9	9	9	9	1	−0.7311	−0.0753	−0.8818	−0.2456
0	9	9	10	10	1	−0.2899	−0.0150	−0.3895	−0.0458
0	9	9	11	11	1	−0.6886	−1.2846	−0.7067	−1.3904
0	10	10	10	10	1	−0.9741	−0.7822	−1.0820	−0.8662
0	10	10	11	11	1	−0.2215	−0.1618	−0.2104	−0.1539
0	11	11	11	11	1	−1.0038	0.0058	−1.2955	−0.3934
0	8	9	8	9	2	−0.9552	−1.0112	−1.0311	−1.0559
0	8	9	8	10	2	−0.1204	−0.2030	−0.0970	−0.1818
0	8	9	9	10	2	0.6284	0.3835	0.6970	0.4181
0	8	10	8	10	2	−1.2568	−1.8634	−1.1987	−1.8466
0	8	10	9	10	2	0.5202	0.2761	0.6037	0.3183
0	9	10	9	10	2	−0.2104	−0.2471	−0.2682	−0.3137
0	8	8	8	8	3	−1.3112	−1.4315	−1.3660	−1.5083
0	8	8	8	9	3	0.3887	0.1360	0.4638	0.1820
0	8	8	9	9	3	−0.0907	−0.2309	−0.0601	−0.2289
0	8	8	9	10	3	−0.0532	0.0844	−0.0490	0.0633
0	8	8	11	11	3	0.3073	0.1825	0.2773	0.1351
0	8	9	8	9	3	−0.3480	−0.4640	−0.3647	−0.4953
0	8	9	9	9	3	0.3857	0.2938	0.4359	0.3210
0	8	9	9	10	3	0.7031	0.6975	0.7771	0.7267
0	8	9	11	11	3	0.0096	−0.1268	−0.0203	−0.1586
0	9	9	9	9	3	−0.3734	−0.3732	−0.4106	−0.4085
0	9	9	9	10	3	−0.6456	−0.3803	−0.7342	−0.3902
0	9	9	11	11	3	−0.2387	−0.3766	−0.2359	−0.4210
0	9	10	9	10	3	−1.2798	−1.2083	−1.3928	−1.2628
0	9	10	11	11	3	−0.1621	−0.1027	−0.1646	−0.1022
0	11	11	11	11	3	−0.3399	−0.0788	−0.4618	−0.2257
0	8	9	8	9	4	−0.9037	−0.7544	−1.0026	−0.8086
0	9	9	9	9	5	−1.4206	−1.4386	−1.5388	−1.5121
0	9	9	11	11	5	−0.1210	−0.1118	−0.1154	−0.1255
0	11	11	11	11	5	−0.2637	−0.2500	−0.2876	−0.2890
0	11	11	11	11	7	−0.4015	−0.5081	−0.3947	−0.5009
0	11	11	11	11	9	−1.3483	−1.5422	−1.4605	−1.6180
1	8	8	8	8	0	−0.8610	−0.8651	−0.6986	−0.9202
1	8	8	9	9	0	−1.2124	−0.5209	−1.1749	−0.5326
1	8	8	10	10	0	−0.8919	−1.0908	−0.8196	−1.1777
1	8	8	11	11	0	1.1606	0.4709	1.1460	0.4327
1	9	9	9	9	0	−1.7203	−0.2369	−1.6333	−0.1462
1	9	9	10	10	0	−0.9609	−0.1705	−0.9277	−0.1558
1	9	9	11	11	0	2.1302	1.7006	2.1771	1.9183
1	10	10	10	10	0	−0.2773	−0.0937	−0.1926	−0.0874

TABLE I *(Continued)*

						Reid pot.		Yale pot.	
T	a	b	c	d	J	Sum	G	Sum	G
1	10	10	11	11	0	0.7296	0.5171	0.7612	0.5595
1	11	11	11	11	0	−1.8301	−0.4183	−1.6625	−0.3496
1	8	9	8	9	1	0.3318	−0.1831	0.3658	−0.2045
1	8	9	8	10	1	0.0537	0.0379	0.0232	−0.0004
1	8	10	8	10	1	0.0440	−0.1319	0.0652	−0.1484
1	8	8	8	8	2	−0.2294	−0.3893	−0.1776	−0.4196
1	8	8	8	9	2	−0.1261	−0.0116	−0.1624	−0.0370
1	8	8	8	10	2	−0.3149	−0.4747	−0.2681	−0.5177
1	8	8	9	9	2	−0.2499	−0.1032	−0.2441	−0.0985
1	8	8	9	10	2	−0.0641	−0.0880	−0.0711	−0.1230
1	8	8	11	11	2	0.3660	0.1422	0.3748	0.1466
1	8	9	8	9	2	0.1955	−0.0405	0.2001	−0.0420
1	8	9	8	10	2	−0.1834	−0.1418	−0.1796	−0.1538
1	8	9	9	9	2	−0.1497	−0.0220	−0.1534	−0.0211
1	8	9	9	10	2	−0.2282	−0.1902	−0.2174	−0.2190
1	8	9	11	11	2	0.3127	0.1978	0.3142	0.2055
1	8	10	8	10	2	−0.3993	−0.7249	−0.3068	−0.7857
1	8	10	9	9	2	−0.4109	−0.1533	−0.3859	−0.1472
1	8	10	9	10	2	−0.3120	−0.2183	−0.3346	−0.2498
1	8	10	11	11	2	0.2793	0.1851	0.3152	0.2070
1	9	9	9	9	2	−0.0516	−0.1960	−0.0544	−0.1923
1	9	9	9	10	2	−0.5081	−0.0794	−0.4968	−0.0560
1	9	9	11	11	2	0.4664	0.3982	0.5135	0.4697
1	9	10	9	10	2	−0.2151	−0.2374	−0.1904	−0.2290
1	9	10	11	11	2	0.4932	0.3528	0.5167	0.3775
1	11	11	11	11	2	−0.6251	−0.4333	−0.6324	−0.4711
1	8	9	8	9	3	0.2681	−0.1960	0.2454	−0.2327
1	8	9	9	10	3	0.1116	−0.0224	0.1331	−0.0206
1	9	10	9	10	3	0.5436	−0.0743	0.5735	−0.0869
1	8	9	8	9	4	−0.1306	−0.3761	−0.0904	−0.3982
1	8	9	9	9	4	−0.3267	−0.0286	−0.3149	−0.0038
1	8	9	11	11	4	0.3627	0.2311	0.3799	0.2498
1	9	9	9	9	4	0.4016	−0.0321	0.4319	0.0064
1	9	9	11	11	4	0.2468	0.2033	0.2680	0.2305
1	11	11	11	11	4	−0.1253	−0.1887	−0.1191	−0.1967
1	11	11	11	11	6	0.0685	−0.1124	0.0558	−0.1127
1	11	11	11	11	8	0.1884	−0.0578	0.2063	−0.0375
0	9	11	9	11	2	−3.1237	−2.7083	−3.1632	−2.7652
0	8	11	8	11	3	−0.6182	−0.3296	−0.6934	−0.3980
0	8	11	9	11	3	0.6963	0.6408	0.7025	0.6106
0	9	11	9	11	3	−1.3826	−1.3948	−1.4118	−1.4431
0	8	11	8	11	4	−0.5587	−0.5601	−0.5750	−0.5785
0	8	11	9	11	4	−0.5073	−0.4777	−0.5231	−0.4697
0	8	11	10	11	4	−0.7688	−0.7746	−0.8282	−0.7980
0	9	11	9	11	4	−0.6904	−0.6502	−0.7715	−0.7179
0	9	11	10	11	4	−0.7313	−0.5882	−0.7647	−0.5886
0	10	11	10	11	4	−1.0554	−1.0326	−1.1205	−1.0810
0	8	11	8	11	5	−0.0209	−0.1013	−0.0135	−0.1104
0	8	11	9	11	5	0.1289	0.1104	0.1406	0.0990
0	8	11	10	11	5	0.2832	0.1051	0.2771	0.0972
0	9	11	9	11	5	−1.1320	−1.1482	−1.1669	−1.1728
0	9	11	10	11	5	−0.7699	−0.6787	−0.7866	−0.6585
0	10	11	10	11	5	−0.5276	−0.5149	−0.5666	−0.5415
0	8	11	8	11	6	−1.4883	−1.5369	−1.6341	−1.6095
0	8	11	9	11	6	−0.6551	−0.5429	−0.7115	−0.5536
0	9	11	9	11	6	−0.3168	−0.3475	−0.3500	−0.3578
0	9	11	9	11	7	−1.6133	−1.6407	−1.6934	−1.6896
1	9	11	9	11	2	−0.6211	−0.3140	−0.6700	−0.3476
1	8	11	8	11	3	−0.5277	−0.4931	−0.5466	−0.5250

TABLE I *(Continued)*

						Reid pot.		Yale pot.	
T	a	b	c	d	J	Sum	G	Sum	G
1	8	11	9	11	3	0.4033	0.1124	0.3998	0.1127
1	9	11	9	11	3	−0.2187	−0.2269	−0.2456	−0.2342
1	8	11	8	11	4	0.1790	−0.0918	0.1448	−0.1059
1	8	11	9	11	4	0.0400	0.0542	0.0361	0.0581
1	8	11	10	11	4	−0.1709	−0.0086	−0.1641	−0.0003
1	9	11	9	11	4	0.0278	−0.2058	−0.0317	−0.2308
1	9	11	10	11	4	−0.1725	−0.0204	−0.1712	−0.0273
1	10	11	10	11	4	0.0770	−0.0895	0.0331	−0.0958
1	8	11	8	11	5	0.0155	−0.1679	−0.0140	−0.1691
1	8	11	9	11	5	0.2205	0.1403	0.2245	0.1513
1	8	11	10	11	5	0.2936	0.2392	0.2842	0.2593
1	9	11	9	11	5	−0.1393	−0.2920	−0.1819	−0.3046
1	9	11	10	11	5	−0.4160	−0.1609	−0.4134	−0.1648
1	10	11	10	11	5	−0.1786	−0.3455	−0.2156	−0.3754
1	8	11	8	11	6	0.2443	−0.0625	0.2357	−0.0539
1	8	11	9	11	6	−0.0109	−0.0133	−0.0120	−0.0195
1	9	11	9	11	6	0.1675	−0.1818	0.0979	−0.2136
1	9	11	9	11	7	−0.7651	−0.9672	−0.7971	−1.0751

Here v^S is the short-range part of the interaction diagonal in l. The separation of the interaction into short- and long-range components is made at the point where the correlated state "heals" to the unperturbed oscillator state. This "healing distance" is denoted by d.

In the formalism, VP is a "pseudopotential" which is added to force healing in those states where the interaction is repulsive and its effect is removed in first order by a subtraction procedure. The pseudopotential is also used in other states to produce healing at any desired distance. It is quite possible to force all the relative wave functions to heal at the same distance, but this is not normally done. It has been shown by Nisley[20] that the matrix elements of the effective interaction are independent of the healing distance when both first- and second-order terms are considered *except* in the $^3S_1$ relative state. However, the second-order contribution of the tensor force in this state is a strong function of the healing distance.

Employing the R potential, when the effective interaction is calculated with an oscillator parameter $b = 2.09$ fm ($\hbar\omega = 9.5$ MeV) and with a healing distance $d = 0.95\times\sqrt{2}$ fm, one finds that the Ca^{40} binding energy is −9.56 MeV per particle corrected for center-of-mass and Coulomb energies. With a healing distance of $d = 1.032\times\sqrt{2}$ fm, the same binding energy is found to be −8.15 MeV per particle. This is to be compared with the experimental result of −8.55 MeV per particle. For the R potential the matrix elements used in this work are those with $d = 1.032\times\sqrt{2}$ fm. It may be added that in making these calculations the contributions of three- and four-body clusters, relativistic effects and true three-body forces have been completely disregarded. For the Y potential, the matrix elements are those of Shakin *et al.*[8,9] with $b = 2.09$ fm and $d = 0.800\times\sqrt{2}$ fm. The calculated binding energy for Ca^{40} with this effective interaction is −7.93 MeV per particle.

Having determined the appropriate healing distances, Eqs. (1)–(7) are employed to calculate the bare matrix elements listed in Table I. These matrix elements on the average differ by 10 to 15% from those supplied to us by Kuo and Brown for the HJ interaction and used in Refs. 13–15 but for some small ones the differences are as large as 100%. It may be appropriate to point out that the method employed by Kuo and Brown is different from the one used here.

It may also be mentioned that the size parameter b used in our calculation corresponds to $\hbar\omega = 9.5$ MeV, consistent with the electron scattering experiments on Ni^{62}, but Kuo assumed $\hbar\omega = 10.0$ MeV.

Effects of Core Polarization

The bare matrix elements, calculated above, do not give good agreement for the spectra of two nucleons outside a closed shell, and it has been found necessary to renormalize these matrix elements in perturbation theory to take into account configurations which are not included in the shell-model treatment. It has been already mentioned that the core-polarization diagrams introduced by Bertsch were shown by Kuo and Brown to give substantial improvement in the calculated spectra.

In calculating the contribution of 3p-1h diagram,

the following particle and hole configurations are included:

p: $1p_{3/2}, 0f_{5/2}, 1p_{1/2}, 0g_{9/2}, 1d_{5/2}, 0g_{7/2}, 2s_{1/2}, 1d_{3/2}$;

h: $0p_{3/2}, 0p_{1/2}, 0d_{5/2}, 1s_{1/2}, 0d_{3/2}, 0f_{7/2}$.

Except when a hole is created in the $0f_{7/2}$ orbit, all p and h excitations need an average energy denominator of $2\hbar\omega$. For the case where a hole is created in $0f_{7/2}$, $\epsilon_h - \epsilon_p = 5$ MeV, seems reasonable. In agreement with Kuo and Brown it is found that the contributions where the hole is made in the $0f_{7/2}$ orbital are important because of the smaller energy denominator. For most cases the strength of various particle-hole contributions are spread out. The two-particle and two-hole corrections to G are made following the work of Kuo and Brown.[1]

The two sets of matrix elements are listed in Table I and on the average agree with each other within 10 to 15% though for some small matrix elements, the differences are quite significant. The differences in the matrix elements influence the energy spectra in a rather complicated manner, and it is therefore difficult to assess the degree of agreement simply by inspection; the resulting energy spectra must be compared.

III. SHELL-MODEL CALCULATIONS

In the last few years a number of shell-model calculations[21-23] assuming a closed Ni^{56} core and valence neutrons in the $1p_{3/2}$, $0f_{5/2}$, and $1p_{1/2}$ orbitals have been reported in the literature. Most of these have been of a phenomenological character; some have used χ^2 fitting of energy-level spectra to determine the two-body matrix elements. Recently some calculations[13,14] with "realistic" HJ nucleon-nucleon potential have given improved fits than the earlier work.[24] Unfortunately the results on Ni^{58} were inadvertently omitted in our published papers[13,14] and are being included here. Though the agreement for the $B(E2)$ values was not encouraging, Auerbach and Cohen *et al.* calculated the ratio $B(E2; 2_2^+ \to 0_1^+)/B(E2; 2_2^+ \to 2_1^+)$ using matrix elements obtained from a fit to energy-level spectra. In Ni^{58} they found the ratio to be about 30 compared with the experimental result of $(1.8 \pm 0.3) \times 10^{-3}$. Similarly for Ni^{60}, in the work of Roy, Raj, and Rustgi,[13] this ratio turned out to be 1.06 and 0.32 in their approximations A' and B' while the experimental value is 0.005. The inhibition of the crossover transition $2_2 \to 0$ as compared with the $2_2 \to 2_1$ transition is not explained because the second excited 2^+ state contains predominantly seniority-2 components, whereas two-phon states should have large seniority-4 components. For similar reasons the small branching ratio $B(E2; 3_1^+ \to 2_1^+)/B(E2; 3_1^+ \to 2_1^+) < 0.004$ is not explained in this calculation.

This rather striking discrepancy has led us to examine the sensitivity of the $B(E2)$ values to the two-body residual interaction used. The Ni^{58} and Ni^{60} calculations are therefore done with two more realistic potentials (Y and R). In a previous study on 1^+ and 3^+ states[15] performed within the MTDA framework, it was found that the $B(E2)$ values are quite sensitive to the matrix elements used.

Ni^{58}

The shell-model calculation for this nucleus which has only two nucleons outside the Ni^{56} core is quite simple and requires only a knowledge of the two-body matrix elements and the unperturbed single-particle energies. Its theoretical description could therefore be used as a testing ground for the $T = 1$ matrix elements. This calculations has been performed for the HJ, Y, and R potentials using the three orbitals $1p_{3/2}$, $0f_{5/2}$, and $1p_{1/2}$, and the effect of $0g_{9/2}$ orbital is also studied. These two sets of results are marked by the numbers 3 and 4 with HJ, Y, and R and are shown in Fig. 1. This notation is used in subsequent figures also.

An examination of Fig. 1 shows that the effect of the $0g_{9/2}$ orbital is quite marked (similar effect is also observed for Cu^{59}) and in general it has the effect of pushing the states up on the average by 0.4–0.55 MeV without affecting the level ordering. All the three potentials give essentially the same level ordering up to about 3 MeV. The ordering of the first 1^+ and 3^+ states for the HJ interaction does not agree with those of Y and R. The results with the three orbitals seem to be better than those with four orbitals, contrary to expectation. A similar effect was noticed previously by Kung, Singh, Raj, and Rustgi[25] in their calculations of Sc^{43} and Ca^{43}, and can be easily understood. With the R potential, for example, the effect of including the $g_{9/2}$ orbital is to depress the ground state from −2.184 to −2.704 MeV while the first excited state is just depressed by 0.046 MeV causing an increased separation between the ground and the first excited state.

On the average the levels of Y3 lie about 0.22–0.27 MeV higher than those of HJ3, while the levels of R3 lie about 0.12–0.23 MeV higher than those of Y3. The calculated spectra for the three interactions seem to have fairly similar deviations with respect to the experimental one.

The first excited 2^+ state for HJ3 is slightly lower and, for Y3 and R3 it is slightly higher than the observed value. The ordering of the experi-

mental levels above the first excited 2^+ state is not reproduced with any of the potentials. For example, in the three- as well as four-orbital approximations, the order of the 4_1^+ and 2_1^+ states is reversed though both these states lie within 0.6 MeV of the observed ones except for the 2_2^+ state calculated with the HJ interaction. The 0^+ state which is always difficult to reproduce is found to lie fairly close to the observed value. The same can be said of the 1_1^+ state which is suspected to lie at 2.90 MeV[26,27] and is much better reproduced by HJ3 as compared to the other two interactions.

The electromagnetic decay properties of Ni^{58} have been studied extensively by Horoshko *et al.*[26] and Bertin, Benczer-Koller, and Seaman.[27] The calculated $B(E2)$ values for the Y and R potentials connecting some of the states are given in Table II under the column SM. One can see from this table that the two interactions give more or less the same results except for $B(E2;\ 3_1^+ \to 2_1^+)$. The branching ratios $B(E2;\ 2_2^+ \to 0^+)/B(E2;\ 2_2^+ \to 2_1^+)$ and $B(E2;\ 3_1^+ \to 2_1^+)/B(E2;\ 3_1^+ \to 2_2^+)$ are 0.54, 0.037 and 0.45, 0.005, respectively, for the Y and R potentials. Auerbach and Cohen *et al.* had also calculated the ratio $B(E2;\ 2_2^+ \to 0^+)/B(E2;\ 2_2^+ \to 2_1^+)$ using matrix elements obtained from their fit to energy-level spectra and both found the ratio to be 30 compared with the experimental result $(1.8 \pm 0.3) \times 10^{-3}$. Our results are much closer to the observed value, though still too high.

Cu^{58}

Cu^{58} is of interest theoretically as well as experimentally for several reasons. It is the heavi-

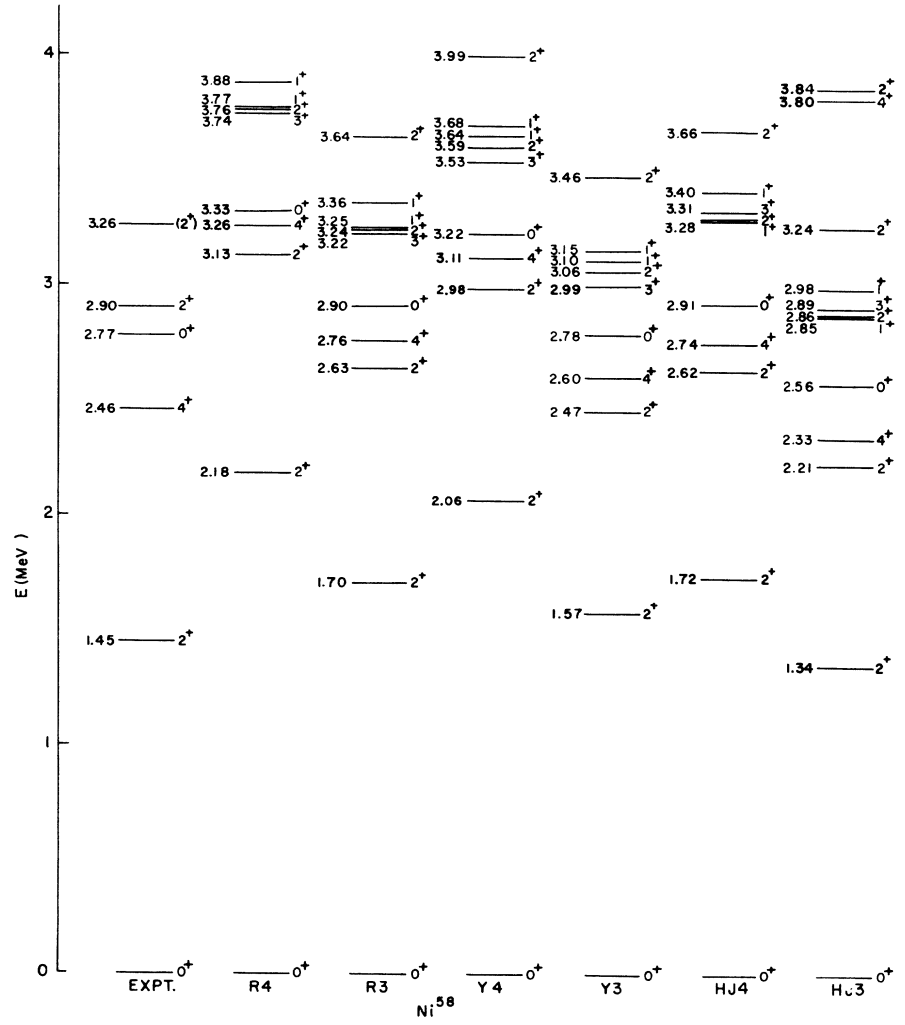

FIG. 1. Comparison of the experimental (Expt) and shell-model spectrum for Ni^{58} employing the Hamada-Johnson (HJ), Yale (Y), and soft-core Reid (R) effective-interaction matrix elements. The integers 3 and 4 denote the number of orbitals included in the calculation.

est known odd-odd nucleus having $N=Z$. Unlike the self-conjugate odd-odd nuclei from Cl^{34} to Co^{54}, with the exception of K^{38}, its ground state is not characterized by superallowed positron transitions to the ground state of neighboring Ni^{58} with $T=T_z=1$. Freeman *et al.*[28] therefore concluded that the ground state of Cu^{58} was not the 0^+, $T=1$ analog state but the 1^+, $T=0$ state. In the Ni^{58}-$(He^3,t)Cu^{58}$ reaction Sherr, Blair, and Armstrong[29] identified the first excited state on intensity grounds as the analog state. The spins and parity of the other levels are not known, though several have been observed[30] in recent years. In Ni^{58}, which is the $T_z=1$ member of the $T=1$ triplet containing Cu^{58}, the first excited state is the 2^+ state at 1.452 MeV. The state in Cu^{58} at 1.638 MeV is just 1.429 MeV above the 0^+, $T=1$ state: One can therefore make a conjecture that this is a 2^+ state.

This nucleus has only one proton and one neutron outside the Ni^{56} core, and hence its theoretical description could be used as a testing ground for the $T=0$ matrix elements with Ni^{56} as core. With this motivation in mind the numerical calculations are carried out for the HJ, Y, and R potentials and the results are presented in Fig. 2. The results show a very negligible effect of the $g_{9/2}$ orbital which is quite different than the one observed in Ni^{58}. The R and Y potentials yield almost identical spectra for the $T=0$ states, but there is a marked difference in the energy of the 0^+, $T=1$ state. The HJ levels, in general, are much lower than the corresponding ones for Y and R but the ordering is almost the same except in one or two cases.

TABLE II. Comparison of shell-model (SM) and Tamm-Dancoff-approximation (TDA) $B(E2)$ values for Ni^{58} using the matrix elements of the Yale and Reid potentials. The $B(E2)$ values are in units of e^2/α^2 where $\alpha=m\omega/\hbar$ is the oscillator parameter.

Reduced transition rate	Yale SM	Yale TDA	Reid SM	Reid TDA
$B(E2;\ 2_1^+\rightarrow 0^+)$	2.146	2.167	2.189	2.233
$B(E2;\ 2_2^+\rightarrow 0^+)$	0.745	0.273	0.703	0.225
$B(E2;\ 2_1^+\rightarrow 2_2^+)$	1.374	0.369	1.511	0.253
$B(E2;\ 3_1^+\rightarrow 2_1^+)$	0.007	0.003	0.001	0.005×10^{-2}
$B(E2;\ 3_1^+\rightarrow 2_2^+)$	0.188	0.022	0.192	0.006

The ground state is reproduced by all three interactions. The first excited 0^+ state is well reproduced in R4. If the level observed at 1.64 MeV is assigned a spin 2^+ with $T=1$, it is well reproduced only by HJ3. All the three interactions predict at least three levels with spins 1^+, 2^+, and 3^+ between the 0^+, $T=1$ and 2^+, $T=1$ states.

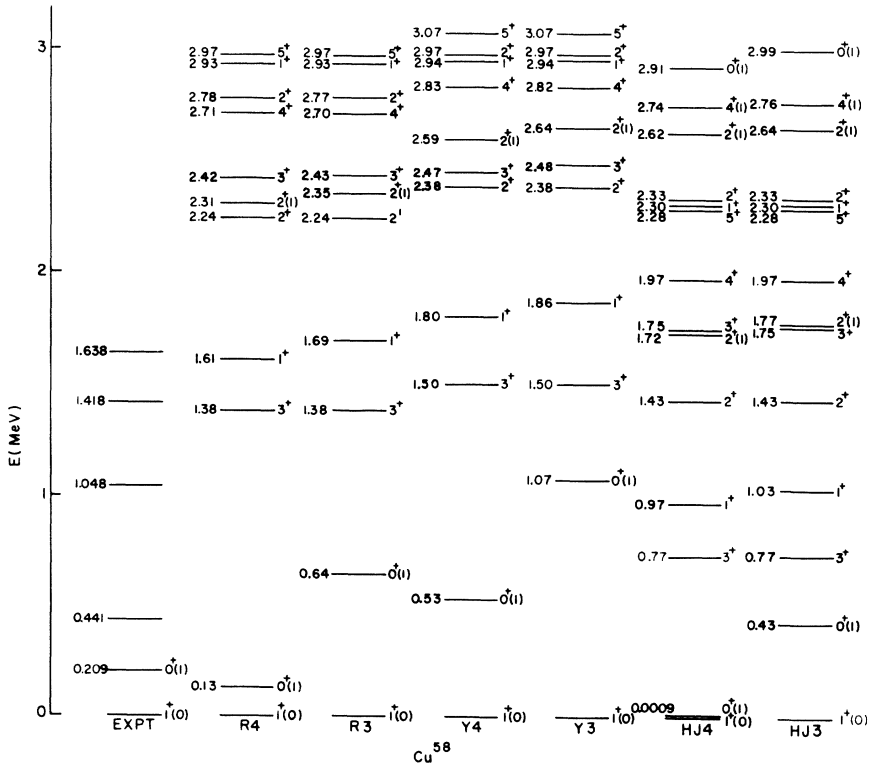

FIG. 2. Comparison of the experimental (Expt) and shell-model spectrum for Cu^{58}.

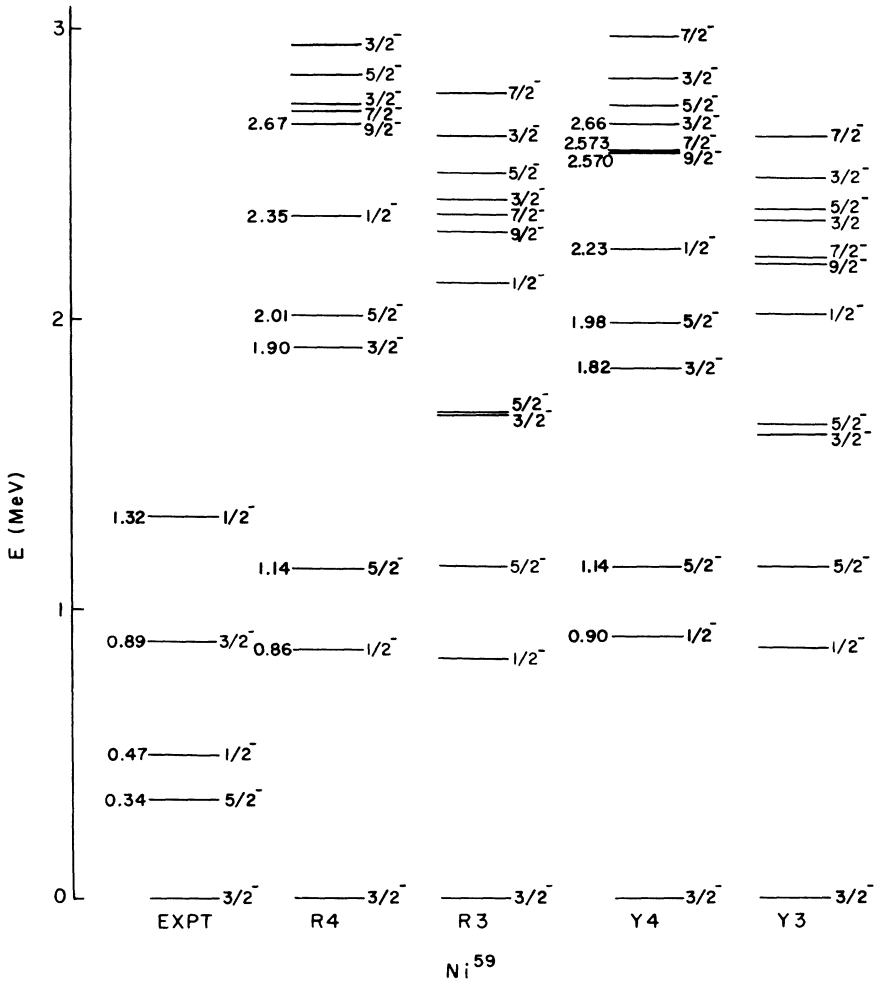

FIG. 3. Comparison of the experimental and shell-model spectrum for Ni^{59}.

TABLE III. Comparison of the $B(E2)$ values for Ni^{60} with the matrix elements of the Yale and Reid potentials. SM denotes the shell-model results and MTDA denotes the quasiparticle results. $B(E2)$ values are in units of e^2/α^2 where $\alpha = m\omega/\hbar$ is the harmonic-oscillator parameter. The entries under the columns $\nu^{J^\pi}_{SM}$ and $\nu^{J^\pi}_{qp}$ represent the percentage admixtures of shell-model seniority-2 and two-quasiparticle states, respectively, for the first state with spin and parity J^π in $B(E2)$.

Reduced transition rates	Yale				Reid			
	SM	MTDA	$\nu^{J^\pi}_{SM}$	$\nu^{J^\pi}_{qp}$	SM	MTDA	$\nu^{J^\pi}_{SM}$	$\nu^{J^\pi}_{qp}$
$B(E2;\ 2^+_1 \to 0^+)$	2.941	3.047	95.13	96.43	2.908	3.114	95.59	97.55
$B(E2;\ 2^+_2 \to 0^+)$	0.696	0.055	91.36	53.17	0.817	0.044	91.94	59.42
$B(E2;\ 2^+_2 \to 2^+_1)$	1.025	1.194			0.959	0.977		
$B(E2;\ 3^+_1 \to 2^+_1)$	0.770	0.003	91.04	74.35	0.795	0.0003	91.26	77.35
$B(E2;\ 3^+_1 \to 2^+_2)$	1.706	0.431			1.703	0.309		

Experimentally also, there are three levels whose spins are not known. The high density of levels between 2 and 3 MeV which is predicted by all three interactions has not yet been observed. Nothing definite could be said about them.

Ni^{59}

The energy level spectrum for Ni^{59} is presented in Fig. 3 for the Y and R potentials. Similar results with the HJ potential have been published before.[14]

It is clear from the Fig. 3 that the ordering of the levels corresponding to Y3, R3 and Y4, R4 is the same and their energies differ very slightly. Unlike the calculation of Ni^{58}, the $g_{9/2}$ orbital has only little effect on the energy levels and has no affect on the level ordering. It can also be seen that the present calculation does not reproduce the experimental ordering and the calculated levels lie relatively high.

Cu^{59}

The energy spectrum for Cu^{59} calculated for the Y and R potentials is shown in Fig. 4. It can be seen from the figure that the first three states agree better in energy with the observed ones for Y4 and R4, compared with the corresponding Y3 and R3 values except the first $\frac{5}{2}^-$ state for Y3. An examination of the figure also shows that the ordering of the levels corresponding to Y3 and R3 and also Y4 and R4 is the same but the results for these two sets differ in energy by more than 0.25 MeV. In general the levels for R lie higher than those of Y. The effect of the inclusion of $g_{9/2}$ orbital is quite marked. In most cases its effect is to push the states up more than 0.25 MeV. Above 1.0 MeV, the spin and parity of the observed states are not known and, therefore, not much can be said about their comparison with the calculated values. In the calculations carried out with the HJ potential and reported in Ref. 14,

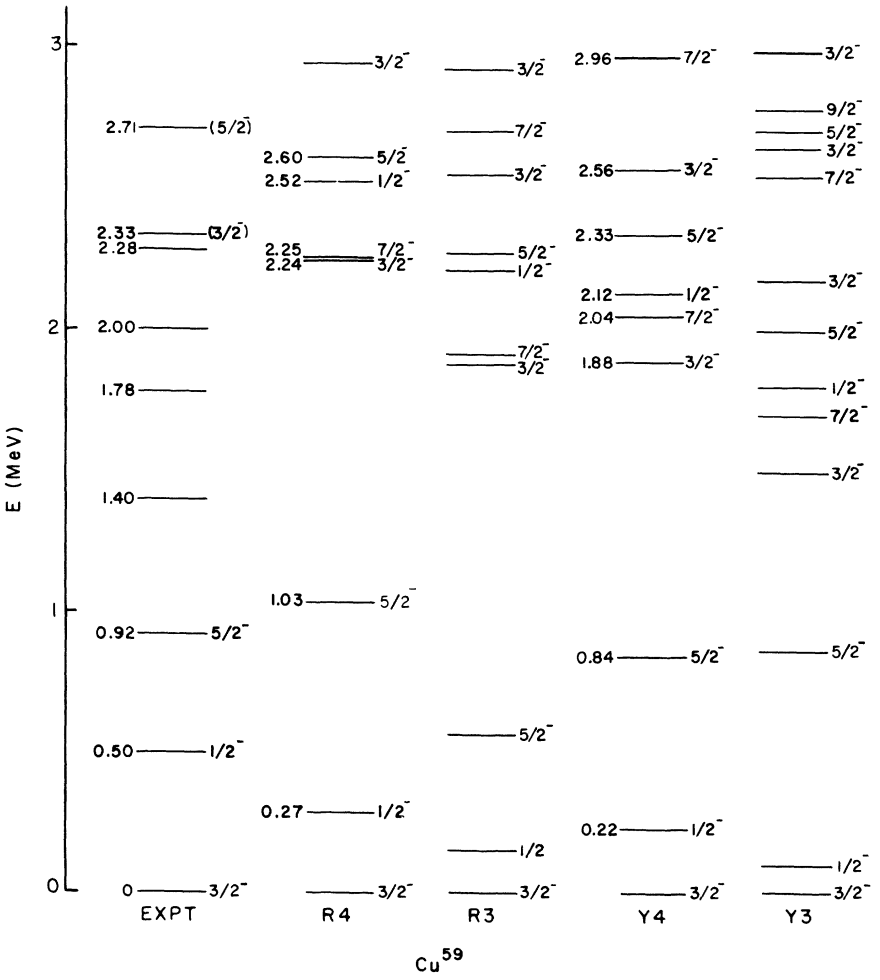

FIG. 4. Comparison of the experimental and shell-model spectrum for Cu^{59}.

the spectroscopic factors for the reaction Ni^{58}-$(He^3, d)Cu^{59}$ were also calculated which reasonably well agreed with the experimental values. A comparison of the wave functions indicates that similar agreement should be expected with the Y and R potentials.

Ni^{60}

The calculated levels of Ni^{60} are shown in Fig. 5, and the results of HJ3 are included for comparison.[13] All the three interactions yield almost identical results. In general the calculated levels lie higher than the observed ones. As for Ni^{59} this calculation also does not reproduce the level ordering above the first excited 2^+ state and describes only the rough trend of the energy spectrum. The similarity of the results for Y3 and R3 is further supported by the $B(E2)$ values calculated between some of the states and are shown in Table III, where the percentage admixture of the seniority-2 component for the 2_1^+, 2_2^+, and 3_1^+ is shown and the results are compared with those obtained by the MTDA method.

The shell-model branching ratio $B(E2;\ 2_2^+ \to 0^+)/B(E2;\ 2_2^+ \to 2_1^+)$ for the Y and R potentials is 0.68 and 0.85, respectively, while the experimental value is 0.005 indicating a vibrational characteristic. An analysis of the wave functions indicates that the second excited 2^+ state contains predominantly seniority-2 components, whereas to ex-

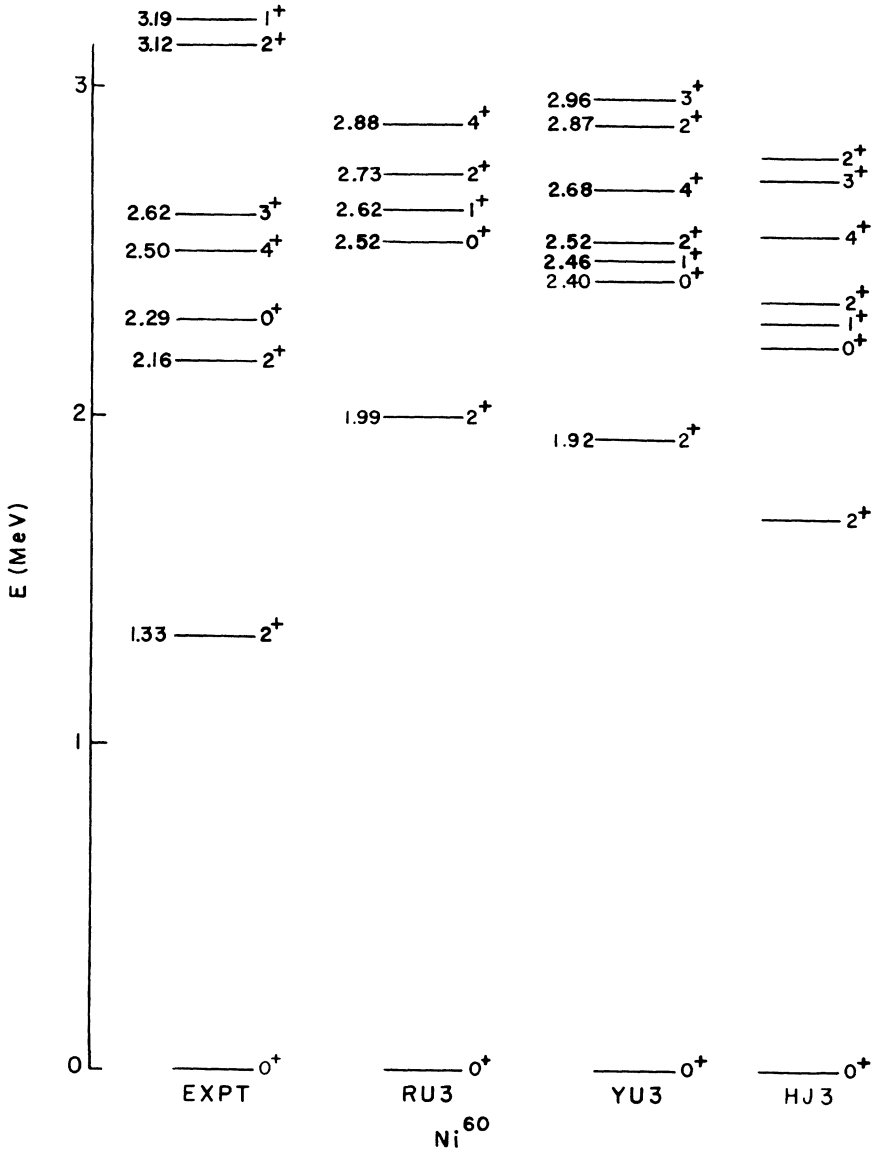

FIG. 5. Comparison of the experimental and shell-model spectrum for Ni^{60}.

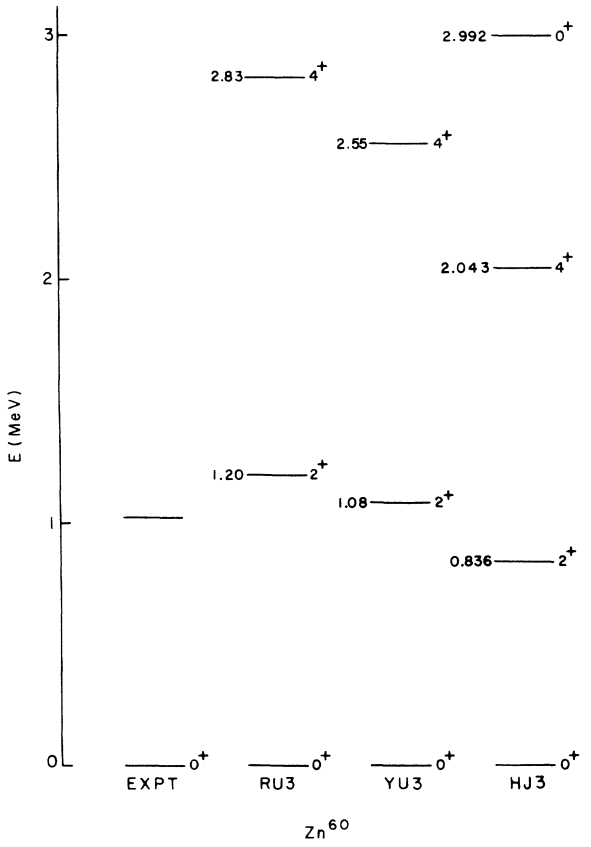

FIG. 6. Comparison of the experimental and shell-model spectrum for Zn^{60}.

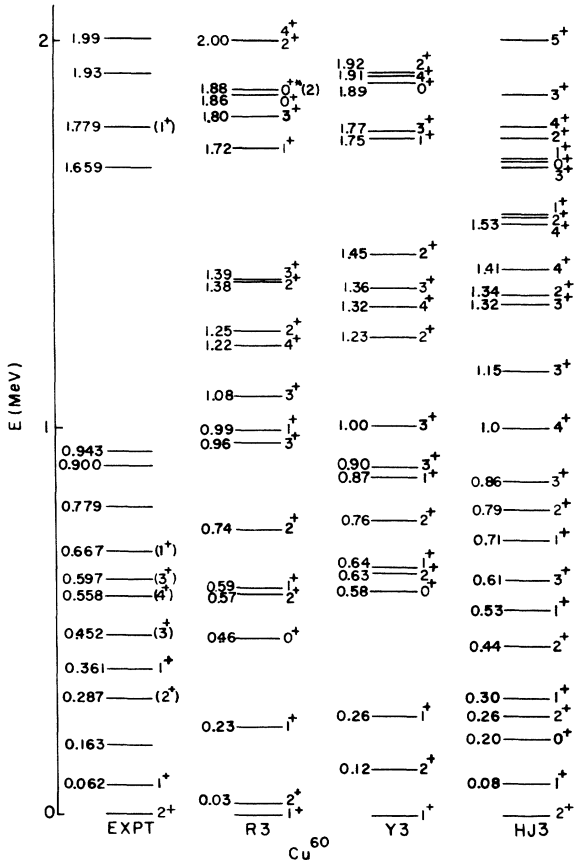

FIG. 7. Comparison of the experimental and shell-model spectrum for Cu^{60}.

plain the above branching ratio it should have large seniority-4 components. The branching ratio $B(E2;\ 3_1^+ \to 2_1^+)/B(E2;\ 3_1^+ \to 2_2^+)$ has also been measured by Van Patter and Mohindra[31] and found to be very small (<0.004). The calculated shell-model values with the Y and R potentials turn out to be 0.45 and 0.47, respectively. This disagreement can again be understood by remembering that our 3_1^+ state wave function is dominant with seniority-2 components.

Zn^{60}

From Fig. 6 one finds that the Y and R renormalized matrix elements reproduce the ground-state spin and their results for the excited states are close to each other and to the HJ3 values published earlier by Singh and Rustgi.[32] The first excited 2^+ state compares well with the unas-

TABLE IV. A comparison of the calculated and observed ground-state binding energies with respect to the Ni^{56} core for the various interactions. In the calculations below, the Coulomb energy for the proton is assumed to be 8.5 MeV.

Isotope	Observed binding energy with respect to the Ni^{56} core	Calculated values Hamada-Johnston	Yale	Reid
Ni^{58}	22.45	22.30	22.47	22.68
Cu^{58}	13.10	14.23	15.05	14.82
Ni^{59}	31.45	32.35	35.59	35.73
Cu^{59}	25.87	26.60	27.09	27.23
Ni^{60}	42.84	44.00	44.03	44.52
Cu^{60}	35.93	37.25	37.83	37.90
Zn^{60}	...	33.15	33.95	34.13

TABLE V. Calculated and experimental energy levels (MeV) of even Ni isotopes for the Yale potential. The rows labeled 4qp (%) and 0qp (%) denote percentage admixture of four- and zero-quasiparticle states, and Exact denotes the results of shell-model calculation. The row TDA (for Ni^{58}) refers to the results obtained in the two-quasiparticle space, while the row MTDA represents the results obtained by mixing zero-, two-, and four-quasiparticle states.

A	J^π	0^+	0_1^+	0_2^+	1_1^+	1_2^+	2_1^+	2_2^+	2_3^+	3_1^+	3_2^+	4_1^+	4_2^+
58	Expt	0.00					1.45	2.78	2.90			2.46	
	Exact	0.00	2.78		3.10	3.15	1.57	2.47	3.06	2.99		2.60	
	TDA	0.00	2.64	3.78	2.83	3.03	1.65	2.39	2.81	2.83	3.99	2.37	3.64
60	Expt	0.00	2.29				1.33	2.16	3.12			2.50	
	Exact	0.00	2.40		2.46		1.92	2.52	2.87	2.96		2.68	
	MTDA	0.00	2.76	3.33	3.01	3.29	2.05	2.70	2.89	3.10	3.46	2.72	3.52
	4qp (%)	13.22	12.03	36.84	22.21	12.33	3.57	46.83	7.94	25.65	54.37	2.65	50.28
	0qp (%)	86.77	0.14	0.13									
62	Expt	0.00	2.05				1.17	2.30				2.34	
	MTDA	0.00	2.98	3.28	3.28	3.56	2.03	2.76	3.17	3.15	3.48	2.94	3.47
	4qp (%)	15.29	14.29	41.76	23.83	17.04	4.92	81.16	22.31	75.50	11.07	9.30	43.42
	0qp (%)	84.70	0.13	0.72									
64	Expt	0.00	2.28				1.34	2.89				2.62	
	MTDA	0.00	3.05	3.35	3.48	3.58	1.96	2.79	3.22	3.24	3.58	3.02	3.59
	4qp (%)	14.54	3.60	46.09	29.84	59.86	1.40	95.60	11.20	41.78	53.71	14.58	6.32
	0qp (%)	85.41	0.53	0.07									
66	MTDA	0.00	2.79	3.30	3.43	3.73	1.74	3.02	3.20	3.09	3.75	2.98	3.59
	4qp (%)	9.23	17.35	46.00	0.58	17.61	0.17	0.90	15.82	1.67	4.43	3.49	1.94
	0qp (%)	90.67	2.23	3.70									

TABLE VI. Calculated and experimental energy levels (MeV) of even Ni isotopes for the Reid potential. For other details see captions of Table V.

A	J^π	0^+	0_1^+	0_2^+	1_1^+	1_2^+	2_1^+	2_2^+	2_3^+	3_1^+	3_2^+	4_1^+	4_2^+
58	Expt	0.00					1.45	2.78	2.90			2.46	
	Exact	0.00	2.90		3.25	3.36	1.70	2.63	3.24	3.22		2.76	
	TDA	0.00	2.74	3.95	3.01	3.27	1.80	2.58	3.01	3.04	4.14	2.53	3.77
60	Expt	0.00	2.29				1.33	2.16	3.12			2.50	
	Exact	0.00	2.52		2.62		1.99	2.73				2.88	
	MTDA	0.00	2.82	3.50	3.23	3.55	2.18	2.88	3.11	3.29	3.64	2.88	3.68
	4qp (%)	13.13	12.67	39.47	16.70	12.50	2.45	40.58	13.73	22.65	51.22	2.35	32.77
	0qp (%)	86.86	0.24	0.64									
62	Expt	0.00	2.05				1.17	2.30				2.34	
	MTDA	0.00	3.05	3.45	3.49	3.81	2.19	2.96	3.32	3.37	3.65	3.09	3.63
	4qp (%)	15.17	10.52	46.84	17.84	15.88	3.87	79.90	23.57	71.88	9.99	7.69	30.18
	0qp (%)	84.83	0.09	0.55									
64	Expt	0.00	2.28				1.34	2.89				2.62	
	MTDA	0.00	3.11	3.50	3.65	3.84	2.10	3.00	3.35	3.44	3.78	3.15	3.72
	4qp (%)	14.38	3.30	49.55	21.60	38.18	1.13	94.97	8.41	34.32	48.14	11.49	3.94
	0qp (%)	85.57	0.71	0.01									
66	MTDA	0.00	2.79	3.33	3.61	3.88	1.88	3.14	3.36	3.26	3.91	3.10	3.72
	4qp (%)	9.14	29.21	45.57	0.59	14.29	0.17	0.93	9.71	1.31	3.99	3.28	2.10
	0qp (%)	90.75	3.48	3.71									

signed spin and parity of the observed one by Miller and Kavanagh[33] at 1019 ± 25 MeV. No other levels have been observed and reported so far in the literature for comparison.

Cu^{60}

The theoretical spectra for Cu^{60} for the Y and R potentials are shown in Fig. 7. The three active orbitals are the same as were taken for the HJ3 calculation.[32] The Y3 and R3 results are quite similar and agree with each other within 0.12 MeV. The ordering of the levels in the two cases agrees up to about 0.75 MeV but above 0.75 MeV the ordering in most cases is reversed. Unlike the HJ interaction, both Y3 and R3 do not reproduce the ground state. In general the Y3 and R3 results seem to be quite different when compared with the HJ3 results. A comparison of the observed and calculated ground-state energies is shown in Table IV.

It is clear that in practically all the cases, the R interaction yields more binding energy but the HJ interaction provides values which come closest to the observed ones. It should, however, be recalled that two different approaches have been used in the calculation of the matrix elements. The work of Kuo and Brown is based on the Brueckner theory but the work of Shakin *et al.*, which is used here for the Y and R potentials, employs the unitary-model approach and does not include G_s. Since G_s is repulsive and is included in the Kuo-Brown matrix elements for the HJ interaction, this explains why the Y and R potentials yield more binding.

IV. QUASIPARTICLE CALCULATIONS, RESULTS, AND DISCUSSION

Numerical calculations of the low-lying states of the Ni isotopes (both even and odd) are performed with Ni^{56} as an inert core and the excess neutrons are allowed to occupy the $1p_{3/2}$, $0f_{5/2}$, and $1p_{1/2}$ orbitals in all possible ways, the unperturbed single-particle energies for which are already given in the Introduction. The two-body effective matrix elements, which go as one of the basic input data for setting up of the energy matrix, are the same as used in the shell-model calculations and correspond to the Y and R potentials.

The other set of input data required for setting up of the energy matrix are the quasiparticle energy and occupation (non-occupation) probability of the various single-particle states which are calculated with the knowledge of the quantities described in the above paragraph. It should be mentioned here that in obtaining these quantities for odd Ni isotopes, the contribution of the extra term in the

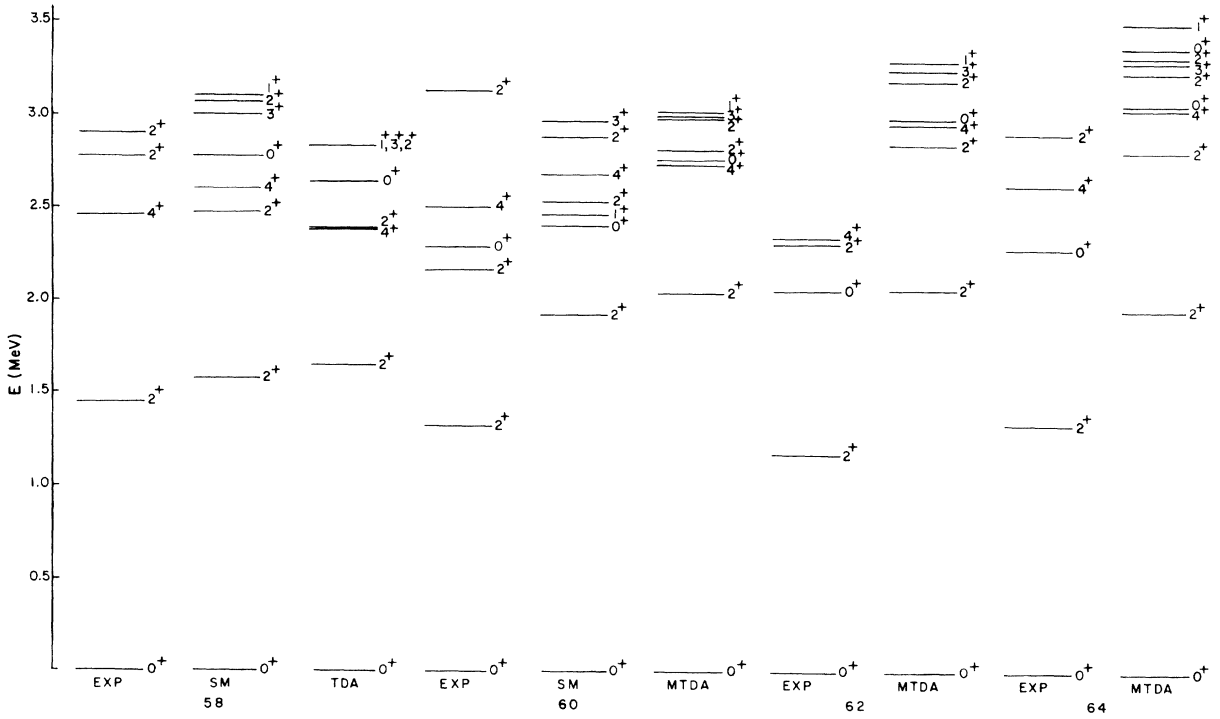

FIG. 8. Comparison of the experimental and quasiparticle (MTDA) spectrum of even Ni isotopes with the Yale potential. SM denotes shell-model results.

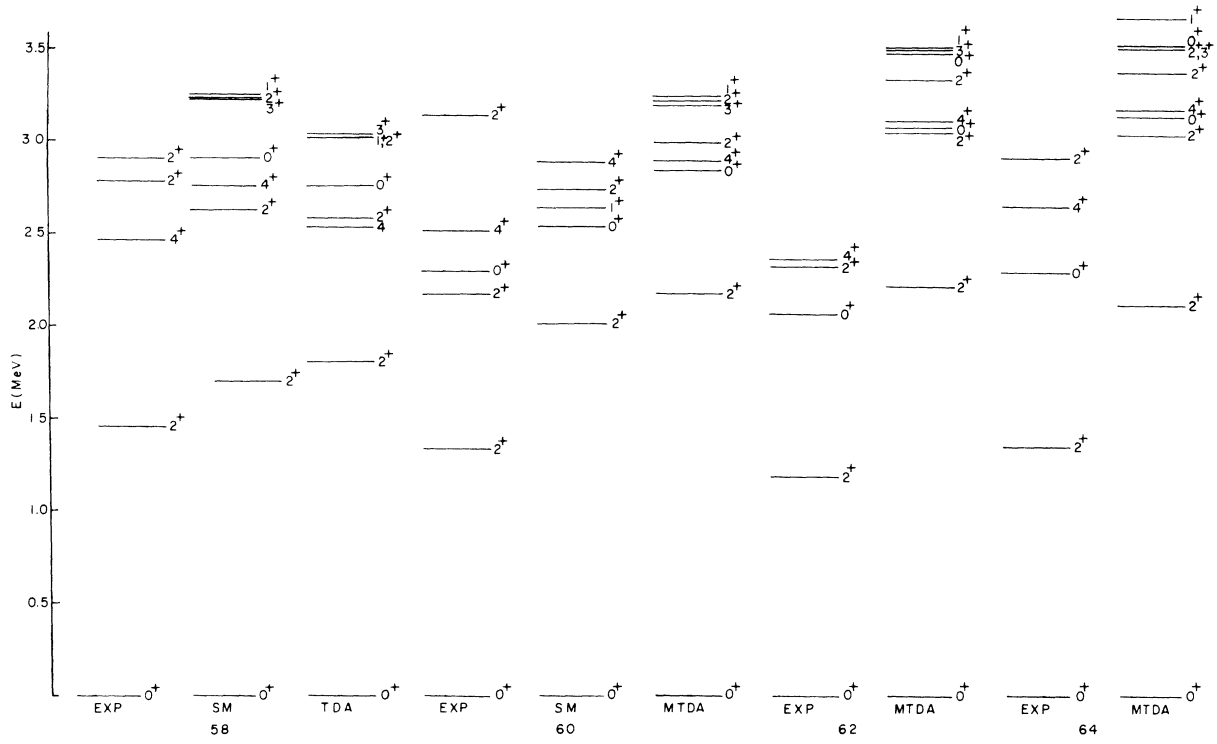

FIG. 9. Comparison of the experimental and quasiparticle (MTDA) spectrum of even Ni isotopes with the Reid potential. SM denotes shell-model results.

BCS equations is also included. The effect of the spurious 0^+ pair state from the basis wave functions is eliminated employing the method given in Refs. 17 and 18, before diagonalizing the energy matrix.

Even Ni Isotopes

The calculated energy levels for the first few states with $J^\pi = 0^+$, 1^+, 2^+, 3^+, and 4^+ for the Y and R potentials are shown in Tables V and VI, respectively. The rows labeled Expt and Exact represent the experimental values and the results obtained by the shell-model calculations. For Ni^{58}, the number of neutrons outside the core being only two, the calculation for this nucleus is restricted to two-quasiparticle states only and the results are shown in the TDA row, while for other isotopes the row MDTA represents the results obtained by mixing the zero-, two-, and four-quasiparticle states, and the percentage admixture of zero- and four-quasiparticle states are shown in the rows marked 0qp (%) and 4qp (%), respectively.

From Tables V and VI one can see that the quality of the agreement between the quasiparticle and shell-model results is almost the same. An examination of these tables also shows that the results for the energy levels for the Y and R potentials are close. In general, the deviation between the two results is quite small, but in some cases

TABLE VII. Comparison of $B(E2)$ values for even Ni isotopes with the matrix elements of the Yale and Reid potentials, calculated by the MTDA method. $B(E2)$ values are in units of e^2/α^2 where $\alpha = m\omega/\hbar$ is the harmonic-oscillator parameter.

Reduced transition rates	Yale				Reid			
	Ni^{60}	Ni^{62}	Ni^{64}	Ni^{66}	Ni^{60}	Ni^{62}	Ni^{64}	Ni^{66}
$B(E2;\ 2_1^+ \rightarrow 0^+)$	3.047	3.012	2.860	2.047	3.114	3.140	2.939	2.075
$B(E2;\ 2_2^+ \rightarrow 0^+)$	0.055	0.195	0.019	0.122	0.044	0.155	0.015	0.126
$B(E2;\ 2_1^+ \rightarrow 2_2^+)$	1.194	1.016	0.528	0.066	0.977	1.088	0.606	0.034
$B(E2;\ 3_1^+ \rightarrow 2_1^+)$	0.003	0.020	0.042	0.010	0.0003	0.021	0.033	0.007
$B(E2;\ 3_1^+ \rightarrow 2_2^+)$	0.431	0.028	0.051	0.405	0.309	0.020	0.031	0.425

it is as much as ≃0.25 MeV. The difference in the percentage admixture of zero- and four-quasiparticle states varies mostly within 10% but in few cases it goes up to about 20%. As regards the dominance of the different quasiparticle components, the two results are almost the same with only few exceptions and the general observations are summarized in the following lines: (1) The ground state has mainly the zero-quasiparticle component with the four-quasiparticle component up to ≃15%. (2) The first excited 2^+ state is predominantly of the two-quasiparticle type with the four-quasiparticle component up to 5%. (3) The first and second excited 1^+ states are of the two-quasiparticle type with the four-quasiparticle component up to ≃30%, with the exception of Ni^{64} for which the Y potential predicts the second excited 1^+ state to be of the four-quasiparticle type with four-quasiparticle component ≃60%, while the R potential predicts it to be of the two-quasiparticle type with the four-quasiparticle component ≃38%. (4) The first excited 0^+ and 4^+ states also have mainly two-quasiparticle component with four-quasiparticle admixture up to within ≃18% except in the case of Ni^{66} for R potential where this admixture is about 29%. (5) The second excited 0^+ and 4^+ states have appreciable four-quasiparticle component in them varying from 37% to approximately 50% except in Ni^{64} and Ni^{66} for which they are predominantly of the two-quasiparticle type and in Ni^{60} and Ni^{62} for the Y potential where the four-quasiparticle component is about 30–33%. (6) The second excited 2^+ state is mainly of the four-quasiparticle type in Ni^{62} and Ni^{64}; Ni^{60} has an appreciable four-quasiparticle component and Ni^{66} is mainly of the two-quasiparticle type, but the third excited 2^+ state is dominantly a two-quasiparticle state with the four-quasiparticle component varying from 8% to ≃23%. (7) The first and second excited 3^+ states are also mostly of the two-quasiparticle type, but in Ni^{64} the four-quasiparticle component is quite appreciable. The first excited 3^+ state of Ni^{62} and the second excited 3^+ state of Ni^{60} are of the four-quasiparticle type with appreciable two-quasiparticle component in them.

A comparison of the experimental and calculated levels is made in Figs. 8 and 9 for the Y and R potentials, respectively. In general, the calculated levels are relatively higher in energy than the corresponding known experimental levels, except for the levels above the 2_1^+ state in Ni^{58}. An examination of these figures shows that even the experimental ordering above the first excited 2^+ state is not reproduced. It should be mentioned that our calculation like others in this mass region provides only the rough trend of the energy spectra.

For Ni^{58} TDA results for the $B(E2)$ values for the Y and R potentials are contained in Table II. One can see that these TDA values are in general, quite different from the corresponding SM values. The calculated branching ratios $B(E2; 2_2^+ \to 0^+)/B(E2; 2_2^+ \to 2_1^+)$ and $B(E2; 3_1^+ \to 2_1^+)/B(E2; 3_1^+ \to 2_2^+)$ are 0.74, 0.14 and 0.87, 0.008, respectively, for the Y and R potentials, and are much closer to the corresponding SM branching ratios compared to the $B(E2)$ values.

For Ni^{60} the calculated $B(E2)$ values for the Y and R potentials, between some of the states are presented in Table III. This table shows that the corresponding $B(E2)$ values are more or less the same for the two interactions. The MTDA results for the branching ratios $B(E2; 2_2^+ \to 0^+)/B(E2; 2_2^+ \to 2_1^+)$ for the Y and R potentials are found to be

TABLE VIII. Calculated and experimental energy levels of odd Ni isotopes for the Yale potential. The row labeled 1qp (%) denotes the percentage admixtures of the one-quasiparticle state. The row Exact is the shell-model results for Ni^{59} and is included for the purpose of comparison.

A	J^π	$1/2_1^-$	$1/2_2^-$	$3/2_1^-$	$3/2_2^-$	$3/2_3^-$	$5/2_1^-$	$5/2_2^-$	$5/2_3^-$	$7/2_1^-$	$7/2_2^-$	$9/2_1^-$
59	Expt	0.47	1.32	0.00	0.89		0.34					
	Exact	0.86	2.01	0.00	1.59	2.33	1.14	1.63		2.20		2.18
	MTDA	0.77	1.87	0.00	1.88	2.13	0.58	1.97		2.24		2.32
	1qp (%)	86.86	7.49	91.32	0.01	3.72	92.65	0.61				
61	Expt	0.28		0.00			0.07	0.91				
	MTDA	0.35	1.33	0.00	1.26	1.74	0.28	1.58	1.77	1.66	1.97	2.13
	1qp (%)	87.57	9.48	91.82	1.73	1.48	94.25	0.66	0.63			
63	Expt	0.00	1.01	0.16	0.53		0.09					
	MTDA	0.00	1.27	0.15	0.64	1.66	0.06	1.37	1.53	1.44	1.66	1.93
	1qp (%)	91.88	4.74	90.03	1.61	4.34	92.74	2.81	0.02			
65	Expt	0.06		0.32	0.70		0.00					
	MTDA	0.00	1.98	0.65	1.05	2.24	0.23	1.81	2.20	1.88	2.25	2.43
	1qp (%)	93.01	1.50	88.88	1.13	1.76	92.76	0.42	0.08			

TABLE IX. Calculated and experimental energy levels of odd Ni isotopes for the Reid potential. For other details see caption of Table VIII.

A	J^π	$1/2_1^-$	$1/2_2^-$	$3/2_1^-$	$3/2_2^-$	$3/2_3^-$	$5/2_1^-$	$5/2_2^-$	$5/2_3^-$	$7/2_1^-$	$7/2_2^-$	$9/2_1^-$
59	Expt	0.47	1.32	0.00	0.89		0.34					
	Exact	0.83	2.12	0.00	1.67	2.41	1.15	1.67		2.36		2.30
	MTDA	0.78	1.99	0.00	2.00	2.23	0.54	2.10		2.42		2.46
	1qp (%)	88.64	5.19	90.64	0.09	3.37	92.31	0.54				
61	Expt	0.28		0.00			0.07	0.91				
	MTDA	0.37	1.44	0.00	1.34	1.85	0.24	1.69	1.80	1.81	2.12	2.22
	1qp (%)	89.65	6.92	91.47	1.33	0.99	94.17	0.64	0.05			
63	Expt	0.00	1.01	0.16	0.53		0.09					
	MTDA	0.00	1.34	0.12	0.73	1.75	0.01	1.37	1.63	1.56	1.78	1.97
	1qp (%)	92.57	3.65	90.53	0.96	3.30	93.35	1.41	0.03			
65	Expt	0.06		0.32	0.70		0.00					
	MTDA	0.00	2.05	0.62	1.16	2.31	0.19	1.87	2.28	2.02	2.37	2.50
	1qp (%)	92.97	1.11	89.32	0.53	1.22	92.59	0.05	0.05			

0.046 and 0.045, respectively, and are in much better agreement with the experimental value (0.005) compared with the shell-model results. This improved agreement comes about because the second excited 2^+ state has quite appreciable four-quasiparticle component though in the shell-model results it mainly had a seniority-2 component. In brief, the interpretation of the cross-over transition $2_2^+ \to 0$ as a two-phonon transfer and the transition $2_2^+ \to 2_1^+$ as a one-phonon transfer agrees better with the MTDA analysis compared with the shell-model one. The agreement for the branching ratio $B(E2;\ 3_1 \to 2_1)/B(E2;\ 3_1 \to 2_2)$ also improves considerably, since the MTDA values are found to be 0.007 and 0.001 for the Y and R potentials while the observed value is <0.004. Again this happens because the 3_1^+ states are found to have an appreciable four-quasiparticle component.

The branching ratio $B(E2;\ 2_2 \to 0)/B(E2;\ 2_2 \to 2_1)$ for Ni^{62} and Ni^{64} is 0.19, 0.036 and 0.14, 0.025 for the Y and R potentials, respectively (Table VII). However, this ratio is considerably larger for Ni^{62} but still they indicate the vibrational characteristics of the 2_2^+ states. On the other hand the branching ratio $B(E2;\ 3_1 \to 2_1)/B(E2;\ 3_1 \to 2_2)$ for Ni^{62} and Ni^{64} for the Y potential is little less than unity and for the R potential it is about unity. Thus the analysis of this branching ratio does not indicate the 3_1^+ state to be a two-phonon type, al-

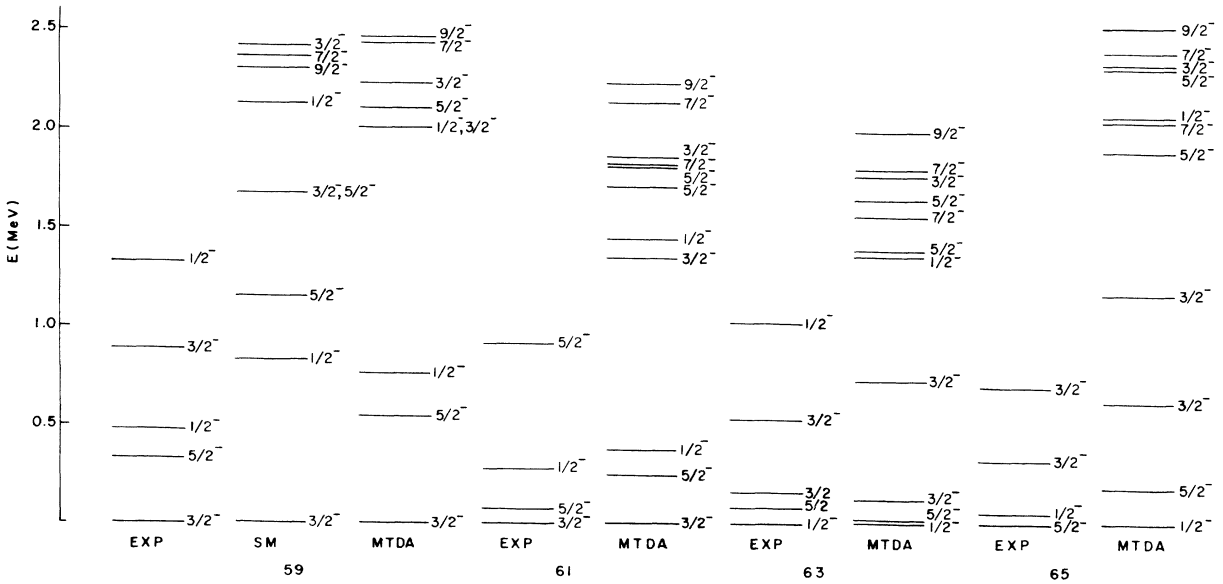

FIG. 10. Comparison of the experimental and quasiparticle (MTDA) spectrum of odd Ni isotopes with the Reid potential. SM denotes shell-model results.

though it is of the four-quasiparticle type. The experimental information for this branching ratio is not known for Ni^{62} and Ni^{64}.

Odd Ni Isotopes

Tables VIII and IX present the results for the energy levels for the Y and R potentials, respectively. All the energy eigenvalues up to the first $\frac{9}{2}^-$ state are included. The row labeled MTDA presents the results obtained by mixing the one- and three-quasiparticle states and the percentage admixture of one-quasiparticle state is represented in the row marked 1qp (%). The row labeled Exact is the results obtained by shell-model method for Ni^{59} and the experimental (Expt) values are shown for the purpose of comparison.

One can notice from Tables VIII and IX that as for even Ni isotopes the results for the energy levels for the two potentials are very close. Mostly the difference between the two results is within 0.13 MeV though in few cases this difference is a little more $\simeq$0.18 MeV such as for the $\frac{7}{2}^-$ and $\frac{9}{2}^-$ states. It is also to be noticed from these tables that the shell-model results for Ni^{59} agree within 0.2 MeV with the MTDA results except for the $\frac{5}{2}^-$ states and the second excited $\frac{3}{2}^-$ state. The results for the percentage admixture of the one-quasiparticle component differ by only a few percent (the maximum difference is $\simeq$5%). The first state of any spin is always predominantly of the one-quasiparticle type with the admixture of the three-quasiparticle component up to $\simeq$12%, the second state is more or less a pure three-quasiparticle state with the one-quasiparticle component up to $\simeq$9%, and the third state (only those reported in Tables VIII and IX) has nearly a pure three-quasiparticle character with the one-quasiparticle component up to $\simeq$4%.

Figures 10 and 11 show that comparison between the experimental and MTDA level spectra for R and Y potentials, respectively. It should be pointed out that for Ni^{59} the MTDA results do reproduce the experimental ordering while the shell-model results do not, although their energies are relatively higher. For Ni^{61}, the ordering of the first three experimental levels is reproduced within reasonable limits but the calculated $(\frac{5}{2}^-)_2$ level lies quite high and also there are two more levels below this level for which there are no corresponding experimental levels. There is quite satisfactory agreement for Ni^{63} between the known experimental levels and the MTDA values. In the case of Ni^{65}, the ordering of the first two levels is reversed and the next two known levels lie slightly higher in energy. A comparison of the wave functions indicate that the results for the $B(E2)$ values will be of the same quality as reported in Ref. 14 for the HJ interaction.

In conclusion we remark that the results obtained by the Y and the R potentials are very similar and they describe the levels of Ni isotopes qualitatively.

The calculation for even Ni isotopes using $1p_{3/2}$, $0f_{5/2}$, and $1p_{1/2}$ orbitals for the Y potential has also been made with the quasiparticle energy and occupation (non-occupation) probability obtained by solving the BCS equations including the $0g_{9/2}$

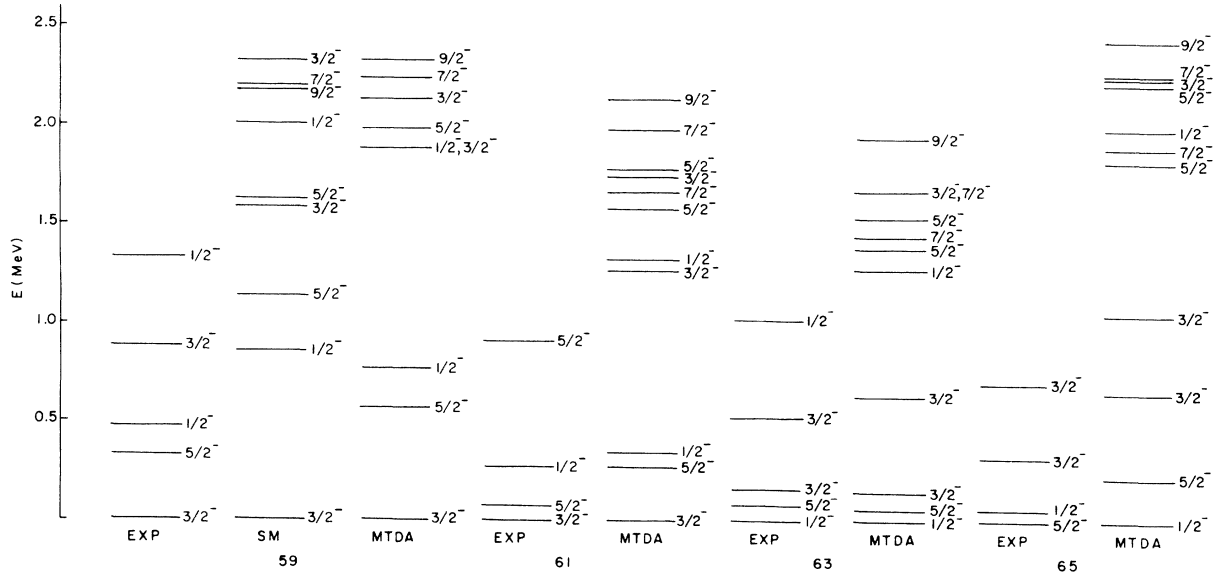

FIG. 11. Comparison of the experimental and quasiparticle (MTDA) spectrum of odd Ni isotopes with the Yale potential. SM denotes shell-model results.

single-particle orbital. The results thus obtained for the low-lying states differ with the one discussed earlier in two respects: (1) The ground state is pushed up approximately by 0.15 MeV, while (2) the excited states are pushed up approximately by 0.7 MeV. Similar results are expected for the R potential. For this reason the calculations were not repeated for the odd Ni isotopes. A similar calculation for the energy levels and transition rates for even and odd Ni isotopes has already been reported for the HJ potential in Refs. 13–15 and showed somewhat better agreement than reported here.

V. CONCLUSIONS

It has often been asserted that different potentials which fit the same two-body scattering data should give essentially the same results for effective-interaction and nuclear-structure calculations. However, no calculations with potentials which differ in shape as much as the soft-core R and HJ or Y potential have been reported in the literature in the nickel region. The predictions of the Y and HJ potentials for the proton-proton scattering data are similar and the two potentials are numerically almost identical. It is found that their effective interactions though calculated by two different methods, agree with each other within 10% or so. The effective interaction due to the R potential agrees within 10 to 15% with the Y or HJ effective interaction. It is found that the three potential models give nuclear-structure results which are quite comparable.[1] On the average, the disparities that do exist indicate that the R soft-core potential is strongest. The HJ potential appears to be the better potential model, giving results closest to the observed values for the spectra as well as for the binding energies. This statement, however, should not be taken literally since it must be recalled that some of the differences in the calculations may have arisen because of the different size parameter and different methods used by Kuo and Brown and by us.

It may also be mentioned that the MTDA calculation describes the vibrational characteristic of the second 2^+ state significantly better compared with the shell-model results. The origin of this improvement is under investigation and will be the subject of a future publication. A calculation of the third-order renormalization effects, not considered here in the evaluation of the matrix elements, is also in progress and its effect on the nuclear-structure calculations will be also soon reported.

Since the completion of this work and submission of our paper for publication, a paper by Jain, Mehta, and Waghmare[34] has appeared in which the interaction of SWTH[6, 9] is used to calculate the effective interaction and energy levels of light and intermediate nuclei (He^6, Li^6, O^{18}, F^{18}, Ni^{58}) and the results are compared with those obtained with the Kuo-Brown matrix elements for the HJ interaction. Jain, Mehta, and Waghmare[34] do not report any results with the R potential and the really common feature between their work and ours is that both the group of workers report $T=1$ matrix elements for the Y potential for the f-p shell region and carry out calculations on the Ni^{58} spectrum. For the HJ interaction Jain, Mehta, and Waghmare[34] employ the Kuo[24] matrix elements which do not include the contribution of G_s, while ours do, and as has been reported earlier, these lead to improved agreement with the observed spectra.[14, 15] For the Y potential, Jain *et al.* use the tables of the relative matrix elements ($\hbar\omega = 9.5$) as given in the paper of SWTH[9] just as we do. However, the differences between the two sets of bare matrix elements may be purely of a computational nature. The core-polarization corrections are different since we treat the $0g_{9/2}$ orbital as active while Jain *et al.* do not do so. This results in some difference in the binding energy. For example, for Ni^{58}, our Y potential matrix elements yield a ground-state binding energy of 22.47 MeV, while Jain *et al.* obtain approximately 21.9 MeV.

It may be mentioned that our core-polarization correction program had been checked to reproduce the published results of Kuo and Brown.[3] The two-body bare matrix elements had been calculated from the relative matrix elements of Shakin *et al.* by two independent computer programs which checked each other to eight significant figures.

ACKNOWLEDGMENTS

The authors take great pleasure in expressing their deep appreciation and gratitude to Professor Gregory Breit for his gentle encouragement, contagious enthusiasm, and numerous illuminating discussions, which are so basic to this and other nuclear-structure work being carried out at Buffalo. Thanks are due to the staff of the computing center of the State University of New York at Buffalo, which is partially supported by the National Institute of Health Grant No. FR-00126 and the National Science Foundation Grant No. GP-7318, for providing the machine time. A grant-in-aid from the Research Foundation of the State University of New York to one of the authors (MLR) is also gratefully acknowledged.

*Work supported by the U.S. Atomic Energy Commission (NYO-4022-17).

[1]T. T. S. Kuo and G. E. Brown, Nucl. Phys. 85, 40 (1966); *ibid.* A90, 199 (1967); R. P. Lynch and T. T. S. Kuo, *ibid.* A95, 561 (1967).

[2]J. F. Dawson, I. Talmi, and J. D. Walecka, Ann. Phys. (N.Y.) 18, 330 (1962).

[3]T. T. S. Kuo and G. E. Brown, Nucl. Phys. A114, 241 (1968).

[4]G. F. Bertsch, Nucl. Phys. 74, 234 (1965).

[5]J. S. Bell, in *Lectures on the Many Body Problem,* edited by C. Fronsdal (W. A. Benjamin, Inc., New York, 1962).

[6]F. Villars, in *Nuclear Physics, Proceedings of the International School of Physics "Enrico Fermi," Course XXIII,* edited by V. F. Weisskopf (Academic Press Inc., New York, 1963).

[7]L. C. Gomes, J. D. Walecka, and V. F. Weisskopf, Ann. Phys. (N.Y.) 3, 241 (1958).

[8]C. M. Shakin, Y. R. Waghmare, and M. H. Hull, Jr., Phys. Rev. 161, 1006 (1967).

[9]C. M. Shakin, Y. R. Waghmare, M. Tomaselli, and M. H. Hull, Jr., Phys. Rev. 161, 1015 (1967).

[10]K. E. Lassila, M. H. Hull, Jr., H. M. Ruppel, F. A. McDonald, and G. Breit, Phys. Rev. 126, 881 (1962).

[11]M. K. Pal and A. P. Stamp, Phys. Rev. 158, 924 (1967).

[12]T. T. S. Kuo, E. U. Baranger, and M. Baranger, Nucl. Phys. 81, 241 (1966).

[13]B. B. Roy, R. Raj, and M. L. Rustgi, Phys. Rev. C 1, 207 (1970).

[14]R. P. Singh, R. Raj, M. L. Rustgi, and H. W. Kung, Phys. Rev. C 2, 1715 (1966).

[15]M. L. Rustgi, B. B. Roy, and R. Raj, Phys. Rev. C 1, 1138 (1970); 2, 2446 (1970).

[16]R. V. Reid, Ann. Phys. (N.Y.) 50, 411 (1969).

[17]M. K. Pal, Y. K. Gambhir, and R. Raj, Phys. Rev. 155, 1144 (1967).

[18]Y. K. Gambhir, R. Raj, and M. K. Pal, Phys. Rev. 162, 1139 (1967).

[19]M. Moshinsky and T. A. Brody, *Tables of Transformation Brackets* (Monografias Instituto de Fisica, Mexico City, Mexico, 1960).

[20]R. A. Nisley, Ph.D. thesis, Oregon State University, 1971 (unpublished).

[21]S. Cohen, R. D. Lawson, M. H. Macfarlane, S. P. Pandya, and M. Soga, Phys. Rev. 160, 903 (1967).

[22]N. Auerbach, Phys. Rev. 163, 1203 (1967).

[23]Y. K. Gambhir and R. Raj, Phys. Rev. 161, 1125 (1967).

[24]R. D. Lawson, M. H. Macfarlane, and T. T. S. Kuo, Phys. Letters 22, 168 (1966).

[25]H. W. Kung, R. P. Singh, R. Raj, and M. L. Rustgi, Phys. Rev. C 1, 1994 (1970).

[26]R. N. Horoshko, P. F. Hinrichsen, L. W. Swenson, and D. M. Van Patter, Nucl. Phys. A104, 113 (1967); P. F. Hinrichsen *et al.*, *ibid.* 81, 449 (1966).

[27]M. C. Bertin, N. Benczer-Koller, and G. G. Seaman, Phys. Rev. 183, 964 (1969).

[28]J. M. Freeman, J. H. Montague, G. Murray, R. G. White, and W. E. Burcham, Nucl. Phys. 65, 113 (1965).

[29]R. Sherr, A. C. Blair, and D. D. Armstrong, Phys. Letters 20, 392 (1966).

[30]J. A. Cookson, Phys. Letters 24B, 570 (1967).

[31]D. M. Van Patter and R. K. Mohindra, Phys. Letters 12, 223 (1964).

[32]R. P. Singh and M. L. Rustgi, Phys. Rev. C 3, 1172 (1971).

[33]R. G. Miller and R. W. Kavanagh, Nucl. Phys. A94, 261 (1967).

[34]M. C. Jain, G. K. Mehta, and Y. R. Waghmare, Phys. Rev. C 3, 1466 (1971).